Molecular Modeling of Zeolite Structure. 2. Structure and Dynamics of Silica Sodalite and Silicate Force Field

John B. Nicholas,*,† A. J. Hopfinger,† Frans R. Trouw,‡ and Lennox E. Iton§

Contribution from the Department of Chemistry, University of Illinois at Chicago, Chicago, Illinois 60680, and the Intense Pulsed Neutron Source Division and Materials Science Division, Argonne National Laboratory, Argonne, Illinois 60439. *Received November 1, 1990*

Abstract: An accurate valence force field for zeolites is presented. The force field contains terms for bond stretches, bond angle bends, dihedral angles, and Lennard-Jones and electrostatic nonbonded interactions. Various treatments of the electrostatics and their effects on the modeling of silica sodalite are discussed. Theoretical infrared (IR) spectra, radial distribution functions, and mean-square displacements are compared to experimental data, demonstrating that the force field accurately reproduces the structure and dynamics of silica sodalite with use of energy minimization, normal mode analysis, and molecular dynamics techniques.

I. Introduction

Zeolites are porous crystals generally composed of Si, Al, and O. They contain channels of molecular dimension, with diameters of 3–10 Å or more. These channels can host a variety of ions, water, and organic molecules. The size selectivity of the channels allows them to act as molecular sieves. Zeolites find wide use in industrial applications. For example, Zeolite A is useful in the separation of linear and branched alkanes. Zeolites are also highly active catalysts and are used in the conversion of methanol to gasoline and the conversion of toluene to benzene and *p*-xylene for the subsequent production of terephthalic acid. The commercial value of zeolites provides motivation to understand their chemistry. This includes the structure and dynamics of the zeolite lattice, the manner in which ions and molecules interact with the lattice, and the actual reaction mechanisms involved in zeolitic catalysis. Molecular modeling, including molecular dynamics (MD) and Monte Carlo simulations, normal mode analysis, energy minimization techniques, and computer graphics, are well suited for studying many of the properties of zeolites. There has been considerable recent interest in applying molecular modeling techniques to the study of zeolites. There have been several recent studies on the dynamics of the zeolite framework.[1-3] The adsorption of alkanes in silicalite was studied by June et al.[4] with Monte Carlo simulation. Lara and co-workers performed a MD study of methane in Zeolite–NaA.[5]

To accurately model the structure and dynamics of the zeolite lattice we must have the correct force field parameters. Since the work on zeolite modeling is very recent, there is still much uncertainty in the valence potentials, Lennard-Jones terms, and charges that comprise a typical molecular modeling force field. This is really not surprising; molecular modeling of organic molecules has been an active area since the 1950's and there is still disagreement between the various force fields. Indeed, the MM2 force field,[6] one of the most widely used, was recently revised.[7] We felt that more accurate valence potentials could be developed for zeolite modeling. In addition, there was a need to investigate the various methods of treating the electrostatic interactions in the zeolite lattice. In prior work[8] we investigated the stability of various forms of the silica sodalite cage and the interactions of ions with the aluminosilicate sodalite. Here we expand on our previous work to simulate the structure and dynamics of the zeolite lattice more extensively and accurately.

II. Theoretical Methods

A. Atomic Positions. We began with silica sodalite, the simplest zeolitic material to model. The truncated cuboctahedral sodalite structure unit is illustrated in Figure 1. The structure is built up by the corner-sharing of SiO_4 tetrahedra to form the 4- and 6-rings of the cuboctahedra. In the silica sodalite framework, all the tetrahedral atoms are silicon, and the composition is SiO_2. Atomic coordinates were taken from a combined single-crystal X-ray and powder neutron diffraction refinement of silica sodalite with encapsulated ethylene glycol.[9] The reported unit cell is cubic, $Im3m$, with $a = 8.83$ Å. This implies that all the silicons and oxygens are equivalent. The refinement suggests that there is some type of inherent structural disorder in the crystal. High-resolution ^{29}Si NMR of this material reveals three peaks.[10] This indicates that there are actually three crystallographically distinct silicons and the true symmetry is lower. Apparently the deviation from cubic symmetry is slight enough that it is not discernable in the diffraction experiment. We assume that the ethylene glycol, which is not included in the simulation, does not have a major effect on the silica sodalite structure.

B. Geometry of the Tetrahedra. Figure 2 illustrates the geometry of the tetrahedra in the sodalite 4-ring using the terminology of Depmeier.[11] For each Si there are six corresponding O–Si–O angles. Two of these angles, termed α, are involved in the 4-rings. The other four angles (α') are part of 6-rings. In the sodalite family the α angle ranges from about 106° to 120° and generally increases with the aluminum content. The tilt angle φ is 0° in silica sodalite, resulting in a planar 4-ring. This is unusual, because in most of the family of sodalites φ ranges from 10° to 40°. When φ is non-zero, the 4-ring is puckered, with alternating oxygens above and below the plane of the Si.

C. Simulation Procedure. The simulation lattice consists of a $2 \times 2 \times 2$ arrangement of unit cells, making the total system a cube of 17.66 Å on each side. The system contains 96 Si and 192 O atoms. Periodic boundary conditions were used to simulate the effects of the infinite framework. The nonbonded interatomic interactions were evaluated for all atoms within a cutoff radius of 8.82 Å. The electrostatic interactions were treated in various ways that will be discussed in detail. Nonbonded Lennard-Jones

* Author to whom correspondence should be addressed.
† University of Illinois at Chicago.
‡ Intense Pulsed Neutron Source Division, Argonne National Laboratory.
§ Materials Science Division, Argonne National Laboratory.

(1) Demontis, D.; Suffritti, G. B.; Alberti, A.; Quartieri, S.; Fois, S.; Gamba, A. *Gazz. Chim. Ital.* **1986**, *116*, 459–466.
(2) Demontis, P.; Suffritti, G. B.; Quartieri, S.; Fois, E. S.; Gamba, A. *Zeolites* **1987**, *7*, 522–527.
(3) Demontis, P.; Suffritti, G. B.; Quartieri, S.; Fois, E. S.; Gamba, A. *J. Phys. Chem.* **1988**, *92*, 867–871.
(4) June, R. L.; Bell, A. T.; Theodorou, D. N. *J. Phys. Chem.* **1990**, *94*, 1508–1516.
(5) Lara, E. C. D.; Kahn, R.; Goulay, A. M. *J. Chem. Phys.* **1989**, *90*, 7482–7491.
(6) Burkert, U.; Allinger, N. L. *Molecular Mechanics*; Caserio, M. C., Eds.; American Chemical Society: Washington, D.C., 1982; p 339.
(7) Allinger, N. L.; Yuh, Y. H.; Lii, J.-H. *J. Am. Chem. Soc.* **1989**, *111*, 8551–8566.
(8) Mabilia, M.; Pearlstein, R. A.; Hopfinger, A. J. *J. Am. Chem. Soc.* **1987**, *109*, 7960–7968.
(9) Richardson, J. W.; Pluth, J. J.; Smith, J. V.; Dytrych, W. J.; Bibby, D. M. *J. Phys. Chem.* **1988**, *92*, 243–247.
(10) Meinhold, R. H.; Bibby, D. M. *Zeolites* **1986**, *6*, 427–428.
(11) Depmeier, W. *Acta Crystallogr.* **1984**, *B40*, 185–191.

0002-7863/91/1513-4792$02.50/0

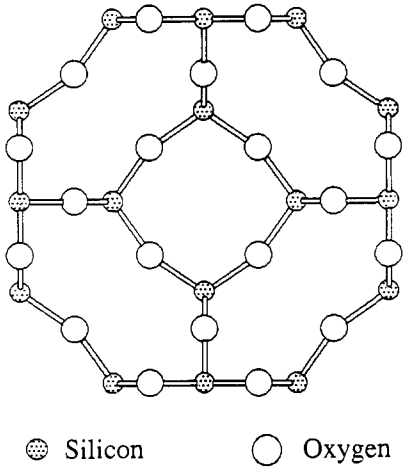

Figure 1. The basic silica sodalite structural unit.

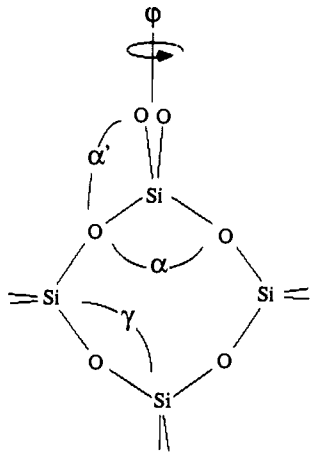

Figure 2. The 4-ring of silica sodalite illustrating the terminology described in the text.

and electrostatic interactions were not calculated for atoms that were bonded (1–2 interactions) or atoms involved in a bond angle (1–3 interactions), as these nonbonded terms are assumed to be accounted for by the bond stretch and bond angle bend potentials. Energy minimizations were performed with conjugate gradients.[12] For the MD simulations the equations of motion for the system were integrated wiwth use of the leap-frog algorithm[13] in a modified version of the program MOLSIM.[14] A MD time step of 1.0 fs was used. Each simulation was equilibrated to 300 K for 20 ps or more by loosely coupling the system to a temperature bath[15] with a temperature relaxation time of 1.0 ps. Following equilibrium, trajectories were computed for an additional 20 ps, during which the atomic positions and velocities were saved for later analysis.

If the nonbonded interactions are simply truncated at the cutoff distance, there is a large discontinuity in the potential. The discontinuity causes a disastrous lack of energy conservation in MD and also hinders convergence in energy minimizations. There are several methods that can be used to smooth the potential and forces to zero at the cutoff distance. We have used the shifted force potential.[16] With the shifted force potential, the total energy of the system in the MD simulations showed no drift and had an average root-mean-square (RMS) fluctuation of 0.6–0.7% of the kinetic energy fluctuations over the entire run, indicating excellent energy conservation.

(12) Gunsteren, W. F. van.; Karplus, M. *J. Comput. Chem.* **1980**, *11*, 266–274.
(13) Hockney, R. W. *Methods Comput. Phys.* **1970**, *9*, 136–211.
(14) Doherty, D.; Hopfinger, A. J. *Macromolecules* **1990**, *23*, 676–678.
(15) Berendsen, H. J. C.; Postma, J. P. M.; Gunsteren, W. F. van.; DiNole, A.; Haak, J. R. *J. Chem. Phys.* **1984**, *81* (*8*), 3684–3690.
(16) Streett, W. B.; Tildesley, D. J.; Saville, G. *Computer Modeling of Matter* **1978**, 144–158.

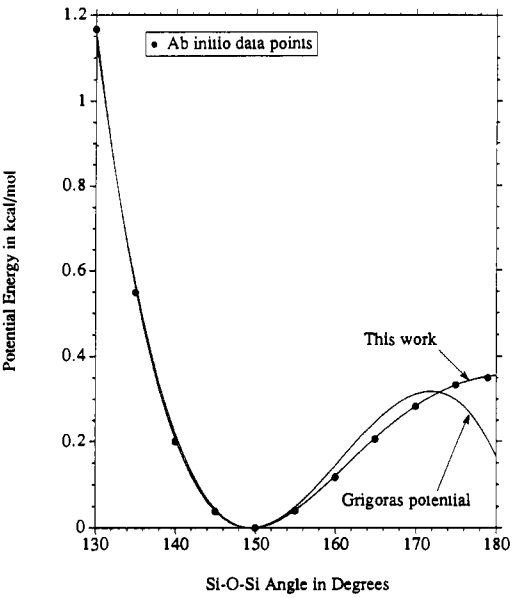

Figure 3. The ab initio Si–O–Si data points and potential fit of Grigoras, compared to the potential fit used in this work.

D. The Force Field. The force field is represented by a sum of potential energy terms

$$V_{total} = V_{bonds} + V_{angles} + V_{torsions} + V_{Lennard\text{-}Jones} + V_{electronics} \quad (1)$$

The values of the force parameters that enter into the potential energy terms can be obtained by a variety of methods. Quantum mechanical calculations on small molecules that mimic the zeolite structure can be used to determine force constants, equilibrium geometries, and charge densities. Fitting the force parameters to experimental data, such as IR frequencies and crystal structures, is also possible and has been used, in part, to derive the force field parameters presented in this work. For example, experimental structural data on a wide range of silicates suggest the following values and ranges for the geometric parameters:[17]

Si–O bond ≈ 1.605 Å (range 1.57–1.72 Å)
O–Si–O angle ≈ 109.5° (range 98–122°)
Si–O–Si angle ≈ 140° (range 120–180°)

(i) **Bond Stretch.** The Si–O bond stretch is modeled with use of a simple harmonic potential

$$V(r) = (k_r/2)(r - r_{eq})^2 \quad (2)$$

where k_r = 597.32 kcal/(mol·Å²) and r_{eq} = 1.61 Å. A considerable range of theoretical values have been reported for the equilibrium Si–O bond length, in addition to the experimentally observed values. SCF calculations[18] of the equilibrium bond length range from ≈1.602 to 1.657 Å. We have found the value of r_{eq} = 1.61 Å to most accurately model the structure and dynamics of silica sodalite. This is very close to the crystallographically observed value and within the range of the theoretical calculations. The effect of various equilibrium bond lengths will be discussed in detail in a later section.

(ii) **Bond Angle Bends.** The O–Si–O bond angle bend is also modeled with a harmonic potential:

$$V(\theta) = (k_\theta/2)(\theta - \theta_{eq})^2 \quad (3)$$

We have used θ_{eq} = 109.5°, the equilibrium angle suggested by observation, and a force constant of k_θ = 138.12 kcal/(mol·rad²).

The Si–O–Si bond angle bend is highly anharmonic.[19] This angle is also known to vary over a range of ≈60° in silicates, three times the amount of variation found in the O–Si–O angle. Thus, we feel that having the correct Si–O–Si potential is very important

(17) Liebau, F. *Structural Chemistry of Silicates*; Springer-Verlag: New York, 1985; p 347.
(18) Sauer, J. *Chem. Rev.* **1989**, *89*, 199–255.
(19) Grigoras, S.; Lane, T. H. *J. Comp. Chem.* **1988**, *9*, 25–39.

to the simulation. On the basis of SCF calculations with an 3-21G* basis set, Grigoras[19] has proposed a potential containing a quadratic and cubic term

$$V(\theta) = (k_{\theta 1}/2)(\theta - \theta_{eq})^2 - (k_{\theta 2}/2)(\theta - \theta_{eq})^3 \quad (4)$$

where $k_{\theta 1}$ = 12.52 kcal/(mol·rad^2), $k_{\theta 2}$ = 21.32 kcal/(mol·rad^3), and θ_{eq} = 149.5° (Figure 3). Grigoras demonstrated that this potential would accurately reproduce the structure of siloxanes in molecular mechanics. Although this potential is a close fit to the ab initio energy over most of the range of the angle, it fits poorly in the 170–180° range. Because the Si–O–Si angle can become linear during the MD simulations, we found it necessary to more accurately fit the ab initio data. The new potential is

$$V(\theta) = (k_{\theta 1}/2)(\theta - \theta_{eq})^2 - (k_{\theta 2}/2)(\theta - \theta_{eq})^3 + (k_{\theta 3}/2)(\theta - \theta_{eq})^4 \quad (5)$$

where $k_{\theta 1}$ = 10.85 kcal/(mol·rad^2), $k_{\theta 2}$ = 22.72 kcal/(mol·rad^3), $k_{\theta 3}$ = 13.26 kcal/(mol·rad^4), and θ_{eq} = 149.5° (Figure 3). This potential gives an excellent fit to the entire range of ab initio data. The equilibrium bond angle of 149.5° is large when compared to the value of 140° suggested by Liebau. However, the experimentally observed angle in siloxane (144.4°) may better represent the equilibrium value. SCF calculations with various basis sets give values for the equilibrium Si–O–Si angle ranging from 124.53° to 180.0°.[20] Clearly, the shallow potential well of this angle makes it a difficult bond to characterize and the ab initio potential calculated by Grigoras seems reasonable. For example, the barrier to inversion of the Si–O–Si bond angle has been determined by Raman spectroscopy to be 0.32 kcal/mol.[21] The ab initio calculations by Grigoras give a barrier of 0.35 kcal/mol, in excellent agreement with the experiment.

(iii) Si–O Bond/Si–O–Si Bond Angle Coupling. In silicates the Si–O bond is known to lengthen as the Si–O–Si bond angle becomes smaller.[22] The exact relationship between the bond length and bond angle depends on the compound and also varies with the amount of Al in the lattice. Hill and Gibbs[23] have proposed the following relationship between the bond and the bond angle in silicates:

$$r_{Si-O} = 1.53 - 0.08/\cos(\theta_{Si-O-Si}) \quad (6)$$

Inspection of the geometry of the crystal structure of silicalite,[24] a zeolite similar to silica sodalite in that it contains only Si and O, results in a slightly different relationship:

$$r_{Si-O} = 1.46 - 0.11/\cos(\theta_{Si-O-Si}) \quad (7)$$

To induce the proper change in the Si–O bond with the Si–O–Si angle in our simulations, we incorporated a Urey–Bradley term based on the Si–Si nonbonded distance for each Si–O–Si angle

$$V(r) = (k_r/2)(r_{Si-Si} - r_{eq})^2 \quad (8)$$

where k_r = 54.6 kcal/(mol·Å), r_{Si-Si} is the distance between the two Si atoms in the Si–O–Si bond angle, and r_{eq} = 3.1261 Å, the distance observed in the silica sodalite crystal structure. In addition to reproducing the correct dynamic behavior of the lattice, we have found that the Urey–Bradley term is needed to obtain the correct separation between the frequencies of the symmetric and asymmetric Si–O stretches.

The Si–O–Si angle exhibits a large equilibrium value when compared to the 110–114° C–O–C angle found in dimethyl ether. One possible cause of the large angle is the overlap of Si 3d and O 2p orbitals. An alternate explanation is that the large Si–O–Si angle is due to steric repulsion between the Si atoms which are in close contact at ≈3.12 Å. In our simulation nonbonded and electrostatic interactions are not calculated between 1 and 3 neighbors. Therefore, the Urey–Bradley term may represent this Si–Si repulsion.

(iv) Dihedral Angle. The torsional potential for the Si–O–Si–O dihedral angle is a periodic function with a 3-fold barrier:

$$V(\Phi) = (k_\Phi/2)(1.0 + \cos(3\Phi)) \quad (9)$$

It is common in a valence force field of this type to assume that torsions appropriate for large systems can be derived from calculations on small, representative molecules.[25] In zeolites we are interested in the energy of rotation about an Si–O bond in an essentially infinite arrangement of SiO_4 tetrahedra. An ab initio calculation of the actual torsional potential in the full zeolite lattice is currently not possible at a reasonable level of sophistication. We must therefore assume that the potential can be derived from compounds such as hydroxysiloxane ($H_3Si-O-SiH_2-OH$) that contain a similar rotatable Si–O bond, with H satisfying the valence on Si, rather than O, as in a zeolite.

Abraham and Grant[20] investigated the rotation about the Si–O bond in hydroxysilane using an STO-3G* basis set. They found a single barrier of 0.68 kcal/mol with a minimum at 0° when the Si and O are eclipsed. Grigoras[19] has also investigated the rotational barrier about the Si–O bond in a variety of siloxane compounds at the 3-21G* level. The torsional barriers for the molecules that exhibit a similar minimum at 0° range from 0.7 to 1.0 kcal/mol. It appears that the main feature of the torsional energy is an ≈0.7 kcal/mol minimum when the Si and O are eclipsed. In adapting this potential to the zeolite, we must consider that O's occupy positions in the zeolite satisfied by H's in hydroxysilane. We would expect a similar interaction between Si and each of these O's, resulting in a 3-fold barrier with minima at the eclipsed conformations. The minima of the torsional potential are in agreement with the *Im3m* crystal structure of silica sodalite, where the dihedral angles are 0°, 120°, and 240°. We have used a force parameter, k_Φ = –0.7 kcal/mol, consistent with both of the ab initio calculations.

Because little distinction can be made between 1–4 nonbonded interactions and explicit torsional potentials, there is a possibility that some nonbonded interactions are being "double counted". There is also a possibility that the torsional potential is "correcting" for some unknown inaccuracy in the Lennard-Jones terms, rather than being an intrinsic feature of the Si–O bond. However, the results of this and other simulations[38,40] do not suggest that the Lennard-Jones terms are in error. In addition, the fact that the ab initio torsional potential is needed to obtain the correct structure (see below) gives further justification to its use. The clarification of this matter will probably require an ab initio determination of the torsional potential in the full zeolite lattice.

As we have previously discussed, both observation and theoretical calculations indicate that it is possible for the Si–O–Si angle to become linear. Since the potential for the Si–O–Si bond angle is continuous through 180°, a linear bond does not in itself present a computational problem. However, is a Si–O–Si angle was to become linear, the dihedral angle containing the linear angle would not be uniquely defined, resulting in a discontinuity in the potential. In practice, the atoms must be linear to the accuracy of the calculation (double precision) for the dihedral angle to be computed incorrectly. Although this appears to be highly improbable, a different problem does occur.

When the Si–O–Si angle is close to linear, it is possible for it to invert, causing a discontinuity in the torsional potential that contains the Si–O–Si angle. Consider a dihedral angle that is in a minimum energy conformation at ~0°. If in the next step of the MD or energy minimization the related Si–O–Si was to invert (Figure 4), the dihedral would now be in a high-energy conformation at approximately 180°. To avoid this discontinuity,

(20) Abraham, R. J.; Grant, G. H. *J. Comput.-Aided Mol. Design* **1988**, *2*, 267–280.
(21) Durig, J. R.; Flanagan, M. J.; Kalasinsky, V. F. *J. Chem. Phys.* **1977**, *66*, 2775–2785.
(22) Genechten, K. A. V.; Mortier, W. J. *Zeolites* **1988**, *8*, 273–283.
(23) Hill, R. J.; Gibbs, G. V. *Acta Crystallogr.* **1979**, *B35*, 25–30.
(24) Koningsveld, H. von.; Bekkum, H. von.; Jansen, J. C. *Acta Crystallogr.* **1987**, *B43*, 127–132.
(25) Hopfinger, A. J.; Pearlstein, R. A. *J. Comp. Chem.* **1984**, *5*, 486–499.
(26) Brooks, B. R.; Bruccoleri, R. E.; Olafson, B. D.; States, D. J.; Swaminathan, S.; Karplus, M. *J. Comput. Chem.* **1983**, *4*, 187–217.

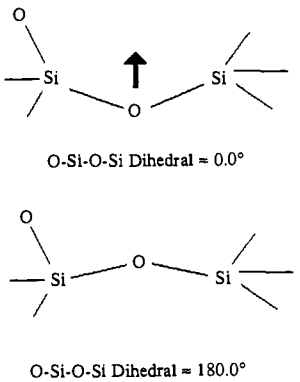

Figure 4. The inversion of the Si–O–Si angle and the effect of inversion on the associated dihedral angle.

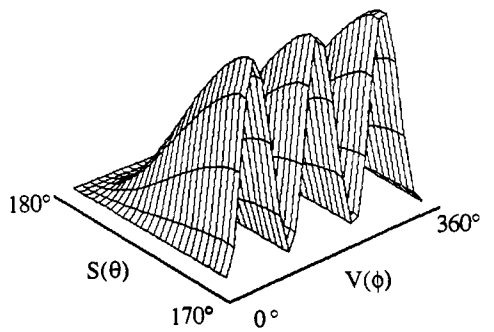

Figure 5. The potential surface of the torsional potential coupled to the switching function. The torsional potential is a periodic function that exhibits minima at 0°, 120°, and 240°. The switching function smooths the torsional energy from its full value to 0 as the related Si–O–Si angle changes from 170° to 180°.

the torsional potential must be coupled to the related Si–O–Si angle, so that the torsional energy goes smoothly to zero as the Si–O–Si bond becomes linear. We have coupled the torsion to a switching function[26] based on the Si–O–Si angle:

$$V(\Phi,\theta) = V(\Phi)S(\theta) \tag{10}$$

where the switching function is defined as

$$S(\theta) = (\theta_{off} - \theta)^2(\theta_{off} + 2\theta - 3\theta_{on})/(\theta_{off} - \theta_{on})^3 \tag{11}$$

$$170° \leq \theta \leq 180°;\ \theta_{on} = 170°;\ \theta_{off} = 180°$$

$$S(\theta) = 1 \qquad \theta < 170° \tag{12}$$

Coupling the torsion potential to the switching function causes the torsional energy to decrease from its full value to zero as the Si–O–Si angle goes from 170° to 180° (Figure 5). In addition to making the potential continuous, smoothing the dihedral to zero for the linear angle seems physically realistic. However, our current use of the switching function is strictly empirical.

(v) Lennard-Jones Terms. Nonbonded interactions were represented in part by a Lennard-Jones 6–12 potential

$$V(r) = B/r^{12} - A/r^6 \tag{13}$$

where r is the interatomic distance. Values for the Lennard-Jones A and B parameters for Si and O were taken from the MM2 force field and are the same as those used in our previous study[8] of zeolites. Lennard-Jones parameters for the Si–O interactions were derived from the usual geometric mean combining rules, i.e. $A_{ij} = (A_iA_j)^{1/2}$.

(vi) Electrostatic Interactions. Nonbonded electrostatic interactions were modeled by a Coulomb potential

$$V(r) = q_iq_j/\epsilon r \tag{14}$$

where q_i and q_j represent the charges of the atoms, r is the interatomic distance, and ϵ is the dielectric constant. The electrostatic interactions are longer range, and can be more important, than the Lennard-Jones terms.

The charges of the zeolite atoms can have an effect both on the structure of the zeolite and on the way ions and molecules interact with the framework. In silica sodalite, the charges arising from the different electronegativities of the silicon and oxygen must be evenly distributed, with the oxygens necessarily having −0.5 the silicon charge. This relationship, in addition to the absence of Al and charge-balancing cations, simplifies the study of the electrostatic interactions. The atomic charges for silicates have been calculated by a variety of methods. Examples of the proposed charge on Si include 0.4[27] and 1.91[22] (electronegativity equilization), 1.0–1.64[28] (CNDO and INDO semiempirical), and 0.69–1.1[19] (SCF/Mulliken). It is evident that there is a wide range of possible values for the Si charge. We have used a Si charge of +1.1 as in our previous study, a reasonable value that is well within the range of the cited calculations.

In addition to the disagreement in the values of the atomic charges, it is also not known which form of electrostatic interaction potential would give the best results in zeolite modeling. The representation of the atoms in the system as point charges is, of course, an approximation. In silica sodalite this approximation is good for the electropositive Si but poor for the more diffuse, polarizable O atoms. The point charge model also ignores the possibility that a significant amount of the electron density may lie between the atoms rather than at the atomic centers. A more detailed treatment of the electrostatic interactions might entail the use of simulated lone pairs on the oxygens and the interaction between bond dipoles, as in the MM2 force field.[6] The large numbers of atoms that are generally needed for zeolite modeling compel us to avoid the increased amount of computation that these addition interactions would require if they are not necessary.

In molecular modeling, it is also usually assumed that nonbonded interactions, both Lennard-Jones and electrostatic, are simply pair-wise additive. Many-body effects and polarization are generally not explicitly included in the simulation. Since polarization always diminishes the electrostatic interactions, the effects of polarization are sometimes crudely approximated by using a dielectric constant that is greater than 1. For organics, a dielectric constant of 3.0–3.5 is often suggested.[29] Grigoras has found that a dielectric constant of 5–8 is needed for the modeling of siloxanes, depending on whether the charges are derived by ab initio or extended Huckel methods.[19] By varying the dielectric constant we are effectively varying the charges on the atoms. This allows us to easily simulate how different charges would affect the system. The simulations were repeated with dielectric constants of 1, 2, and 5.

The discontinuity at the cutoff distance can cause difficulties with convergence in energy minimizations and energy conservation in MD. Initial simulations, without the shifted force potential, would invariably diverge. The shifted force potential, and the incorporation of a cutoff distance, is a useful and necessary approximation that allows the inclusion of the electrostatic interactions in the simulation. However, this also introduces some error because the electrostatic interactions beyond the cutoff distance are assumed to be zero.

The Ewald summation was used to determine what effect the inclusion of the long-range electrostatics would have on the simulation.[30] In the Ewald summation the electrostatic interactions are divided into two rapidly convergent sums, one of which is evaluated in real space while the other is summed in reciprocal space:

$$V = \frac{1}{2}\sum_i^N\sum_j^N\left(\sum_{|n|=0}^{\infty} q_iq_j\frac{\text{erfc}\,(\kappa|\mathbf{r}_{ij}+\mathbf{n}|)}{|\mathbf{r}_{ij}+\mathbf{n}|} + (1/\pi L^3)\sum_{\mathbf{k}\neq 0} q_iq_j(4\pi^2/k^2)\exp(-k^2/4\kappa^2)\cos(\mathbf{k}\cdot\mathbf{r}_{ij})\right) \tag{15}$$

(27) Sanderson, R. T. *Chemical Bonds and Bond Energy*; Academic Press: New York, 1976; p 138.
(28) Sauer, J.; Deininger, D. *Zeolites* **1982**, *2*, 114–120.
(29) Hopfinger, A. J. *Conformational Properties of Macromolecules*; Horecker, B., Kaplan, N. O., Marmur, J., Scheraga, H. A., Eds.; Academic Press: New York, 1973; p 339.
(30) Allen, M. P.; Tildesley, D. J. *Computer Simulation of Liquids*; Oxford University Press: Oxford, 1987; pp 155–162.

Table I. Force Field Parameters

Valence Potential Parameters

Si–O Bond Stretch

$k_r = 597.32^a$ $r_{eq} = 1.61^b$

O–Si–O Bond Angle Bend

$k_\theta = 138.12^c$ $\theta_{eq} = 109.5^d$

Si–O–Si Bond Angle Bend

$k_{\theta 1} = 10.85^c$ $k_{\theta 2} = 22.72^e$ $k_{\theta 3} = 13.26^f$ $\theta_{eq} = 149.5^d$

Urey–Bradley Term

$k_r = 54.6^a$ $r_{eq} = 3.1261^b$

Si–O–Si–O Torsion

$V_3 = -0.70^g$

Nonbonded Potential Parameters

atom	A^h	B^i	charge
Si	2514.1821	9730572.0000	1.1
O	192.8247	158994.0156	−0.55

[a] kcal/(mol·Å²). [b] Å. [c] kcal/(mol·deg²). [d] deg. [e] kcal/(mol·deg⁴). [f] kcal/(mol·deg⁶). [g] kcal/mol. [h] kcal·Å⁶/mol. [i] kcal·Å¹²/mol.

This convergence of the two sums is controlled by the Ewald parameter κ and the range of k-vectors over which the reciprocal space sum is calculated. A value of $5.6/L$, where L is the length of the periodic box, is usually suggested for κ. This was found to be the optimal value for our simulations. The reciprocal space summation was over all k-vectors, $k = 2\pi/L(n_x, n_y, n_z)$, such that n_x, n_y, and n_z are less than 5 and $(n_x^2 + n_y^2 + n_z^2) \leq 27$. The reciprocal space sum includes interactions of the charge of an atom with itself. This is corrected by subtracting from the energy the self term

$$(\kappa/\sqrt{\pi})\sum_{i-1}^{N} q_i^2 \tag{16}$$

In addition, it is necessary to correct the reciprocal sum for the interactions between 1–2 and 1–3 neighbors.[31] These interactions are simply left out of the direct space sum. To correct the reciprocal space sum a term of the form

$$\frac{1}{2}\sum_{i}^{N}\sum_{j}^{N}\left(q_i q_j \frac{\text{erf}\,(\kappa|\mathbf{r}_{ij}|)}{|\mathbf{r}_{ij}|}\right) \tag{17}$$

for the interactions of all 1–2 and 1–3 neighbors i and j is also subtracted from the potential energy. The Ewald summation is computationally expensive. Since the summation system is cubic, some computational simplifications can be made. However, the Ewald summation still increases the amount of cpu time needed for the calculations by approximately 50%.

The complete set of force field parameters is given in Table I.

III. Results

A. Energy Minimizations. (i) Overall Structure. An important measure of the accuracy of the force field is its ability to duplicate the silica sodalite crystal structure. For each treatment of the electrostatics, minimizations were performed with use of the crystal structure as the initial atomic coordinates. The systems were minimized by using conjugate gradients until the gradient norm was less than 1.0 e^{-7}·kcal/(mol·Å). Table II shows the values of the structural parameters of the minimum energy geometry and the percent difference in energy between the initial crystal structure and the minimized geometry, for each of the different treatments of the electrostatics.

In all cases, the minimized geometries are very close to the crystal structure. From the values of the structural parameters, we can see that a dielectric constant different than unity gives a small improvement in the geometry. The experimentally observed Si–O bond length is attained with a dielectric constant of 5. The correct angles are given by a dielectric constant of between 1 and 2. However, such small differences in the geometry can also easily be effected by a slight variation in the other force field parameters, and are not significant. The change in energy on minimization is also very slight; the largest change in energy is less than 0.1% of the total energy of the system. The inclusion of the long-range forces with the Ewald summation has little effect on the structure and gives a structure that is very similar to that obtained with a Coulomb potential and a dielectric of 1. The results indicate that the geometry of the system is primarily determined by the valence potentials and is relatively insensitive to the choice of atomic charges or charge interaction.

Table II. Optimized Geometries and the Percent Change in Energy between the Initial and Final Coordinates for the Different Treatments of the Electrostatics[a]

electrostatics	Si–O	O–Si–O	Si–O–Si	ΔE
Ewald	1.585	109.96	160.05	0.003
$\epsilon = 1$	1.585	110.11	159.89	0.003
$\epsilon = 2$	1.586	110.52	159.48	0.011
$\epsilon = 5$	1.587	110.76	159.24	0.078
expt	1.587	110.3	159.7	

[a] Bond lengths in Å, angles in deg.

Table III. Optimized Geometries and the Percent Change in Energy between the Initial and Final Coordinates for Different Values of r_{eq} in the Si–O Bond Potential[a]

r_{eq}	Si–O	O–Si–O	Si–O–Si	ΔE
1.59	1.583	109.28	160.72	6.650
1.60	1.584	109.68	160.32	2.310
1.61	1.585	110.11	159.89	0.003
1.62	1.586	110.55	159.45	0.669
expt	1.587	110.3	159.7	

[a] r_{eq} and bond lengths in Å, angles in deg.

We have presented results for minimizations starting with the crystal structure. The same geometries are obtained if minimizations are performed on configurations taken from the dynamics trajectories or those that had the atomic coordinates randomly displaced. No alternative energy minima were found.

(ii) The Si–O Bond. The Si–O–Si bond angle is very sensitive to the length of the Si–O bond. For a fixed Si–Si distance, a change of 0.01 Å in the Si–O bond results in an ≈3° change in the Si–O–Si angle. The Si–O–Si angle is thus also very sensitive to the value of the r_{eq} force parameter for Si–O bond stretch. Because of the importance of the Si–O r_{eq} distance and the uncertainty in its optimal value, we performed energy minimizations using a range of Si–O r_{eq} values. Note the value chosen for r_{eq} is not necessarily the value that the Si–O bond will assume in the energy-minimized structure, due to the interaction with the other terms in the force field. Table III shows the change in the geometry of the energy-minimized structures as the equilibrium bond length is changed from 1.59 to 1.62 Å.

The Si–O r_{eq} of 1.59 Å results in an α angle that is less than α', in disagreement with the crystal structure. The change in the α angle with r_{eq} suggests that a value between 1.61 and 1.62 Å would be appropriate. The percent change in energy of the minimized structures also indicates that the r_{eq} value of 1.61 Å causes the least amount of strain in the geometry. Therefore, the optimal r_{eq} value for the Si–O bond is very close to 1.61 Å.

The consequence of increasing the equilibrium bond length is to increase the Si–O bond energy, causing strain about the tetrahedra. An 0.01-Å change in the equilibrium bond length results in a large change in the Si–O potential energy compared to the other energy terms. The strain caused by the longer Si–O bond can be relaxed by a rotation which changes the tilt angle φ. When the torsional potential is not used in the energy minimization the structure develops a twist angle of 12–13°. Thus, the torsional potential predicted by the ab initio calculations is needed in the force field to maintain the correct tilt angle (0°) in silica sodalite. The increase in potential energy associated with the longer equilibrium bond length is similar to the situation that would occur

(31) Heyes, D. M. *CCP5 Quart.* **1983**, *8*, 29–36.

Table IV. Results of Simulation Dynamics: Mean Square Displacements (MSD) of the Atoms from Their Equilibrium Positions, Isotropic Coefficients, and Root-Mean-Square (RMS) Differences between the Average Dynamic Positions and the Crystal Structure

	MSD[a]	isotropic coeff		RMS[b]
		Silicon		
Ewald	0.0040	0.51	0.79	0.0021
$\epsilon = 1$	0.0041	0.51	0.77	0.0023
$\epsilon = 2$	0.0063	0.53	0.78	0.0051
$\epsilon = 5$	0.0116	0.46	0.72	0.0106
expt	0.0163			
		Oxygen		
Ewald	0.0121	0.22	0.76	0.010
$\epsilon = 1$	0.0125	0.21	0.78	0.009
$\epsilon = 2$	0.0182	0.21	0.67	0.010
$\epsilon = 5$	0.0284	0.23	0.42	0.018
expt	0.0369			

[a] Å^2. [b] Å.

when Al is present in the lattice, due to the longer Al–O bond compared to Si–O. Experimentally, it has been observed that as the amount of Al in the sodalite increases, φ also generally increases. For example, a close relative to silica sodalite, TMA sodalite,[32] has a Si/Al ratio of 5 and a tilt angle of $\approx 8°$. The change in φ when Al is introduced into the zeolite should provide additional information for calibration of the torsional barrier.

B. Molecular Dynamics. (i) Mean-Square Displacements and Detailed Motion of the Oxygens. The effects of the electrostatic interactions on the dynamic behavior of the zeolite can be seen by examining the mean-square displacements (MSD's) of the atoms from their equilibrium positions. The MSD's have been calculated from the 20-ps MD trajectories, sampled every 0.1 ps. The results, presented in Table IV, are the average for all the Si and O atoms in the system. Also given in Table IV are the isotropic coefficients.[33] Both of the isotropic coefficients are equal to one if the atomic motion is isotropic. As the atomic motion becomes more anisotropic, the coefficients approach zero. The MSD's of the O atoms are approximately twice that of the Si atoms, and the isotropic coefficients for the O atoms are smaller, indicating that the O atoms undergo a larger and more anisotropic motion. Both of these results agree with the reported crystal data.[9]

The calculated MSD's are smaller than the reported experimental values. However, there is disorder in the crystal that would tend to raise the experimental values. In addition, any uncertainty in the crystal refinement will also increase the MSD's. The accuracy of the MSD's is generally much lower than the accuracy of the structure. Thus, it is not surprising that the calculated MSD's are smaller than the experimental values. The MSD's increase as the dielectric constant is increased. Clearly, by reducing the strength of the electrostatic interactions the atoms are allowed more motion. This is in agreement with a similar treatment of dielectric effects in proteins.[34]

The experimentally determined thermal ellipsoids of O in Si–O–Si bonds are highly anisotropic, and indicate that the larger motion is perpendicular to the Si–Si vector, with smaller motion parallel to the Si–Si vector. Figure 6 is a scatter plot of the positions of the O atoms of a 4-ring in relation to the positions of the Si during the trajectory. The origin of the plot is the center of the Si–Si distance with the Si–Si vector perpendicular to the plane of the paper. The x coordinate indicates motion in and out of the ring with the center of the 4-ring to the left. The y coordinate indicates motion above and below the plane of the ring. The average position of the O's (and/or the crystal position) is indicated with the O. Note that since we are plotting the O position in relation to the Si's which are also moving, the fluctuations do not exactly correspond to the MSD's of the atoms. Still, this plot gives a good indication of the average motion of the O's. Notice that the displacements toward and away from the center of the ring are similar to those above and below the plane of the ring. This is consistent with the experimental thermal ellipsoids. At various times during the simulation the O can be found inside the ring, which in some cases is due to the inversion of the Si–O–Si bond.

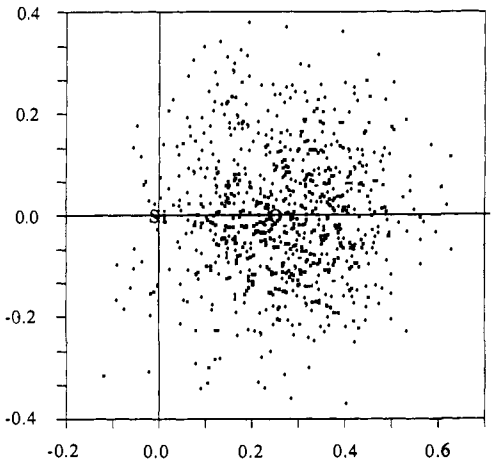

Figure 6. Scatter plot of the positions of the O relative to the Si in a typical 4-ring for motion in and out and above and below the plane of the ring.

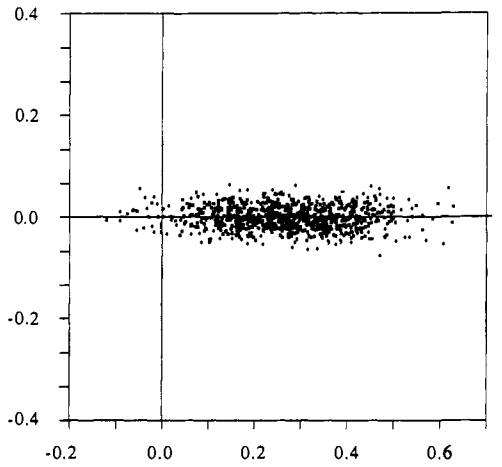

Figure 7. Scatter plot of the positions of the O relative to the Si in a typical 4-ring for motion parallel and perpendicular to the Si–Si vector.

Figure 7 is another plot of the O motion, where the plane of the 4-ring is in the paper, the x direction indicates motion of the O's perpendicular to the Si–Si vector, in and out of the ring, and the y direction is motion parallel to the Si–Si vector. Again the O indicates the crystal position of the O. The motion perpendicular to the Si–Si vector is much less than the parallel motion, consistent with the experiment.

Also included in Table IV is the RMS deviation of the simulated structure from the crystal coordinates. To obtain the RMS deviations, the trajectories were sampled in the same manner as the MSD's, and the average structure was calculated. The average structure was then aligned with the crystal structure[35] and the RMS difference was calculated. The values of the RMS deviations presented are averages over all the Si and O in the lattice. Similar to the MSD's, the trend is for the RMS deviations to increase as the dielectric constant is increased. However, in all cases, the average dynamic structure is very close to that of the crystal, indicating that there is minimal distortion of the lattice during the molecular dynamics simulations.

(32) Baerlocher, v. C.; Meier, W. M. *Helv. Chim. Acta* **1969**, *52*, 1853–1860.
(33) Northrup, S. H.; Pear, M. R.; McCammon, J. A.; Karplus, M. *J. Mol. Biol.* **1981**, *153*, 1087–1109.
(34) Loncharich, R. J.; Brooks, B. R. *Proteins: Struct., Funct., Genet.* **1989**, *6*, 32–45.
(35) McLachlan, A. D. *J. Mol. Biol.* **1979**, *128*, 49–79.

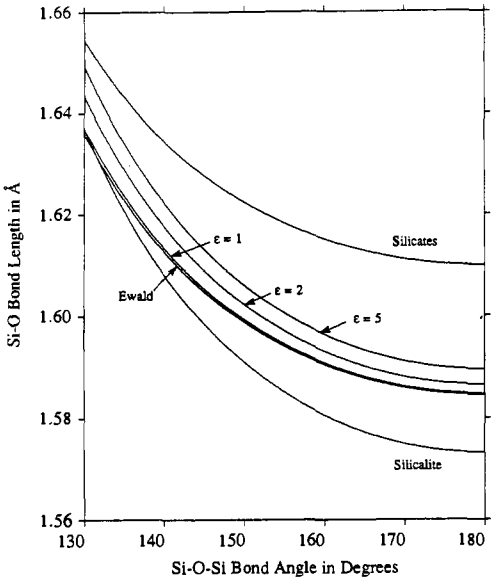

Figure 8. Curves representing the average Si–O bond length versus the Si–O–Si bond angles that are observed during the simulation. Plotted for comparison are the relationship proposed by Hill for silicates and the curve derived from the silicalite crystal structure.

Table V. IR Frequencies (cm^{-1}) of Silica Sodalite Calculated from MD Simulation and Normal Mode Analysis Compared to Experimental Values[a]

	MD	NMA	expt
ring	*b*	302	289
O–Si–O	456	481	450
Si–O sym	776	796	787
Si–O asym	1106	1108	1107

[a] Calculated with the Ewald summation. [b] Frequency cannot be reliably determined.

(ii) Si–O Bond Length/Si–O–Si Bond Angle Coupling. Figure 8 is a plot of a least-squares fit of the average Si–O bond lengths for each of the values of the related Si–O–Si bond angle that occurred during the MD simulations. The values were calculated from the 20-ps MD trajectories, sampled every 0.05 ps. Also plotted for comparison are the relationships proposed by Hill[23] and the curve that we have calculated from the silicalite crystal structure.[24] All of the simulations display realistic bond length/angle coupling that is intermediate between the two experimental curves.

(iii) Simulated IR Spectrum. The IR spectrum was calculated from the molecular dynamics trajectory by the Fourier transform of the total dipole correlation function.[36] The dipole components of the system were calculated every femtosecond over 5 ps of the simulation. Multiple time origins were used in calculating the dipole correlation function, and the spectrum was then smoothed with a 5-point filter. The intensities obtained by this method are qualitative because the quantum corrections needed to give completely accurate intensities are impractical for such a large system.

The IR spectrum was also calculated from a normal mode analysis (NMA) with use of the energy minimized structures discussed previously. For the NMA, intensities are derived from the change in the dipole moment of the system that is associated with the atomic displacements of each normal mode. The frequencies calculated from the NMA are not exactly the same as those that are obtained from the MD. This is because the MD allows the actual anharmonic motion of the atoms to take place, whereas the NMA assumes harmonic motion.

Table V compares the peaks in the experimental IR spectra[37] with those from the MD simulation and the NMA. The results

(36) Berens, P. H.; Wilson, K. R. *J. Chem. Phys.* **1981**, *74* (9), 4872–4882.
(37) Beest, B. W. H. v.; Man, A. J. M. d.; Jackson, R. A.; Catlow, C. R. A.; Santen, R. A. v. *Zeolites; Facts, Figures, Future* **1989**, 763–772.

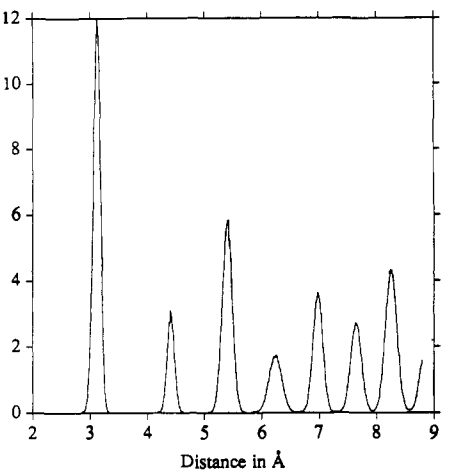

Figure 9. Si–Si radial distribution function. Distances in Å.

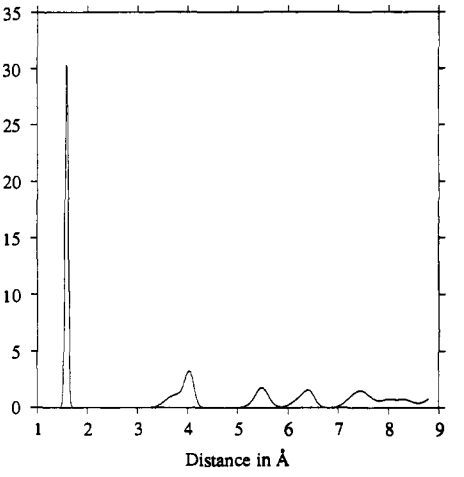

Figure 10. Si–O radial distribution function. Distances in Å.

are presented for the simulations that use the Ewald summation. Because the spectrum depends largely on the valence potentials, the other treatments of the electrostatic interactions give very similar results. Both the MD and normal mode peaks match the experiment very well. The peak at ≈300 cm^{-1} that is obtained with the NMA cannot be reliably discerned in the MD spectrum.

(iv) The Internal Pressure. Under the conditions of static equilibrium, the net force, the moments of the force, and the stress in a crystal must equal zero at equilibrium. In terms of the simulation, this implies that if the system is truly at equilibrium, the potential functions put no net strain on the system. The system should not expand or contract. A simple way to test this is to calculate the internal pressure of the system with use of the virial theorem. In MD this is done with

$$P = Nk_bT/V - \langle \sum r_i \cdot F_i \rangle / 3V \qquad (18)$$

where P is the pressure, N is Avogadro's number, T is the temperature of the simulation, V is the volume of the system, and the quantity in brackets represents the long-term average sum of the atomic positions and forces. Large, high-frequency fluctuations in the internal pressure require that averages be taken over relatively long (20 ps or more) simulations to get an accurate representation of the true pressures. In these simulations, the long-term average pressure tended toward 0, indicating that the system was at equilibrium. Another test of the stress on the cell is to subject the cell to minimizations that allow the sides of the cell to change. These minimizations resulted in changes of less than 1% in the lattice constants.

(v) Radial Distribution Functions. Figure 9 shows the radial distribution function (RDF) for the Si–Si interatomic distances calculated from the MD trajectory. Results are presented for the simulation that used the Ewald summation. The rigid nature of

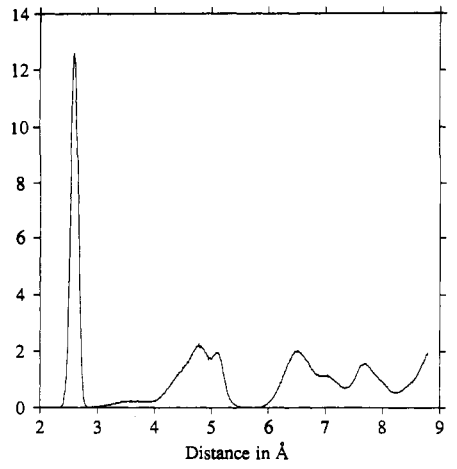

Figure 11. O–O radial distribution function. Distances in Å.

the zeolite framework and the small mean-square displacements of the Si give the Si–Si RDF sharply defined peaks out to the cutoff distance. The peaks in the RDF are all within ±0.1 Å of the interatomic distances that are predicted by the crystal structure. The RDF for Si–O (Figure 10) displays a much different character due to the larger and more anisotropic motion of the O. The first peak at ≈1.57 Å is well-defined, corresponding to the Si–O bond distance. At larger separation, the RDF is much smoother and approaches 1. The RDF for O–O (Figure 11) similarly shows a sharp peak at the first neighbor distance only.

IV. Discussion

The force field presented in this work extends the MM2 formalism to zeolites and has been shown to give a complete and accurate description of the structural and dynamic behavior of silicia sodalite. The force field is practical for molecular modeling studies of the zeolite framework and also can be used in modeling the interaction of adsorbed molecules and ions with the zeolite.

The most notable previous attempts to simulate the zeolite lattice were those of Demontis and co-workers.[1-3] Their force field contained only harmonic and anharmonic terms that represented bond stretches and angle bends. Although a valence force field of this nature is computationally economical for long MD simulations, we feel that the more complete force field presented in this work is needed for several reasons.

First, the interaction of adsorbed ions and molecules with the zeolite is through electrostatic and dispersion interactions. Although this work does not show any strong dependence on the nonbonded terms, by including these terms in the current force field, we demonstrate that they are at least a reasonable representation of the true nonbonded interactions in the zeolite. The extension of the simulation to include adsorbates is easily accomplished because the Lennard-Jones terms for a wide range of atom pairs are readily available in the MM2 force fields, from which our values for Si and O were taken. The results of modeling adsorbate interactions in the zeolite with these additional MM2 nonbonded potentials will be presented in the following paper in this series.[38]

The inclusion of dihedral angle potentials in the force field has been shown necessary to maintain the correct conformational behavior of the lattice, primarily the positions of the O's. Because the dominant feature of adsorption is the interaction of the adsorbed ions and/or molecules with the O's in the lattice, the accurate positioning of the O's is very important. Of course, the widespread use of torsional potentials in other valence force fields also argues for their importance. The coupling of the torsional potentials to the switching function allows them to be used in a computationally tractable and chemically realistic manner. This approach should be found valuable in other molecules that contain the highly flexible Si–O–Si bond, such as siloxanes.

(38) Nicholas, J. B.; Trouw, F. R.; Iton, L. E.; Hopfinger, A. J. Submiitted for publication.

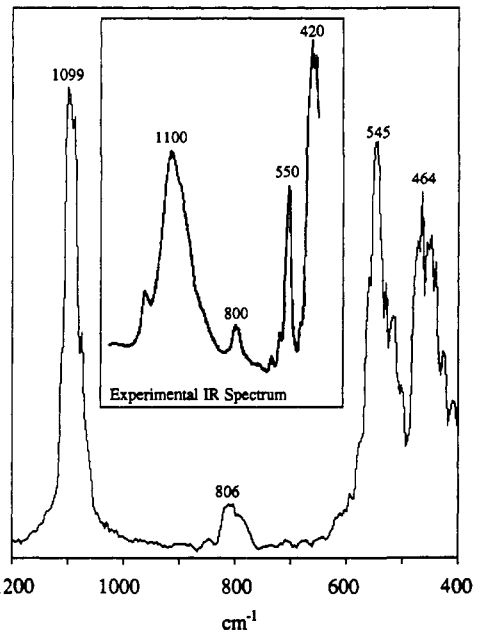

Figure 12. Calculated IR spectrum of silicalite. Inset: experimental spectrum.

Despite our assumptions that the electrostatics could play an important part in the simulation of silica sodalite, we instead found little effect. The geometries of the energy-minimized structures were slightly improved by an increase in the dielectric constant. However, the differences in geometry were negligible, and on that basis it would be difficult to justify a reduction in the electrostatic interactions. The MSD's also suggest a decrease in the charges might be warranted; however, if the experimental MSD's are inflated by as little as a factor of 2, the calculated values are in agreement with the computed values. We do not believe that there is conclusive evidence for a decrease in the charges. We also observed little difference in structure or dynamics when the long-range interactions were included with the Ewald summation. If the long-range interactions were truly unimportant we could benefit by not having to use the computationally intensive Ewald summation in further simulations.

There are several reasons why the electrostatics interactions play less of a role in the structure and dynamics of silica sodalite than might be expected. First, silica sodalite is a special case because of its cubic symmetry. Every Si or O atom is in an identical environment, and therefore has the same average interaction with all the neighboring atoms. In addition, all the individual Si and O carry the same charge and the O must have a charge of $-q_{Si}/2$ to maintain overall charge neutrality. Thus the charge symmetry of the system is fixed and the only possible error is in the actual magnitude of the charges or the failure to include lone pairs or higher order terms. In zeolites of lower symmetry, all Si and O would not have the same charge, and this charge asymmetry will make the structure and dynamics much more sensitive to the effects of the electrostatic interactions. Of course, the substitution of Al in place of Si would leave the lattice with a net charge and cause an even greater charge asymmetry. Because of this high structural and charge symmetry, any errors in the nonbonded interactions will tend to cancel. Thus, silica sodalite does not present a sensitive test of the nonbonded interactions in zeolites. The simulation of lower symmetry and Al-containing zeolites will give much more insight into the correct treatment of the electrostatic interactions and will be presented in future papers.

Finally, each group of two oxygens and one silicon is charge neutral and can be thought of as a charge group.[39] Electrostatic

(39) Gunsteren, W. F. v.; Berendsen, H. J. C. *Groningen Molecular Simulation (GROMOS) Library Manual*; Biomos: Nijenborgh 16, Groningen, The Netherlands, 1987; pp 1–229.

interactions between neutral charge groups fall off as $1/r^3$ rather than $1/r$, diminishing the strength of their long-range interactions. Although we choose not to calculate the electrostatic interactions using the charge group formalism, doing so could be an effective alternative to the shifted force potential in reducing the discontinuity in the potential at the cutoff distance.

Although our force field is very complete when compared to previous zeolite valence force fields, it contains only classic types of potentials that have been commonly included in molecular mechanics force fields. Thus, the force field is chemically realistic and does not contain any artificial terms that could only be used to improve the sodalite results. We have argued that the number of terms in the force field presented here is needed for accurate zeolite modeling. We therefore do not believe that the force field represents an overfitting to the experimental data of silica sodalite, which would result in a force field that reproduces silica sodalite with high accuracy, but models other zeolites poorly. The verification of these claims is the demonstration of the transferability of the force field to other systems. In addition, as a simple matter of convenience, we would like to be able to simulate other zeolites with minimal or no changes in the force field. Figure 12 compares the experimental and theoretical IR spectra of silicalite.[40] The theoretical spectrum was calculated by using the force field presented here and is in excellent agreement with experiment. The transferability of the force field to silicalite is persuasive evidence that the valence force field is valid for silicate zeolites in general.

(40) Nicholas, J. B.; Mertz, J.; Trouw, F. R.; Iton, L. E.; Hopfinger, A. J. Submitted for publication.

V. Conclusion

An accurate force field for the modeling of silicate zeolites has been presented. The force filed contains terms that represent both the valence and nonbonded interactions of the zeolite. The force field has been demonstrated to reproduce the structure and dynamics of silica sodalite with use of energy minimization, normal mode analysis, and molecular dynamics techniques. The transferability of the force field to silicalite has been shown, and the extension of the force field to the study of the interaction of adsorbates with the lattice is easily accomplished. The derivation of additional force field parameters that will allow the inclusion of Al, P, and other metals in the framework is currently being pursued and will be reported in subsequent papers in this series.

Acknowledgment. We would like to thank Dr. William Smith, S.E.R.C. Daresbury Laboratory, Daresbury, U.K., Dr. Mark McAdon, Dow Chemical Company, Midland, Michigan, and Dr. John Mertz, Cray Research, Inc., Mendota Heights, Minnesota, for their helpful discussions. We would also like to thank Dr. Smith for providing the CCP5 computer code, on which our Ewald summation was based. The simulations were performed on an Alliant FX-8 at the Theoretical Chemistry Group, Argonne National Laboratory, Argonne, Illinois, and we thank Dr. Thom Dunning, Jr., and Dr. Albert Wagner for making the computer time available. We also acknowledge the resources of the Laboratory of Computer-Aided Molecular Modeling and Design at the University of Illinois at Chicago. Portions of this work were funded by the U.S. Department of Energy, BES-Material Sciences, under contract No. W-31-109-ENG-38.

Role of Solvent Reorganization Energies in the Catalytic Activity of Enzymes

Arpita Yadav,[†] Richard M. Jackson,[‡] J. John Holbrook,[‡] and Arieh Warshel*,[†]

Contribution from the Department of Chemistry, University of Southern California, Los Angeles, California 90089-1062, and Department of Biochemistry, University of Bristol Medical School, Bristol BS8 1TD, U.K. *Received November 2, 1990*

Abstract: The catalytic reaction of lactate dehydrogenase (LDH) is examined by microscopic simulations for the general class of hydride-transfer reactions in enzymes. The free energy surfaces for the enzymatic reaction and the corresponding reference reaction in solution is evaluated by the empirical valence bond (EVB) method combined with a free energy perturbation method. The resulting activation barriers (Δg^*) are then analyzed in terms of the corresponding solvent reorganization energies (λ_s) by using linear free energy type formulation but with microscopically deduced parameters. It is found that λ_s is smaller in the enzyme than in solutions and that the reduction of Δg^* by the enzyme can be correlated with the corresponding reduction of λ_s. This result, which can be formulated by a Marcus-type relationship, is not, however, reproduced by macroscopic models that consider active sites as low dielectric regions. In fact, nonpolar sites would reduce λ_s but at the same time *increase* rather than decrease Δg^* for charge-transfer reactions. Apparently, enzymes accelerate reactions by using very polar sites with preoriented dipoles. This means that, in contrast to the customary case in homogeneous solutions, where Δg^* can be reduced in nonpolar solvents due to the reduction in λ_s, enzymes can reduce Δg^* by having a small λ_s in a polar environment. This rather complicated situation requires one to evaluate λ_s by microscopic models rather than to estimate it by macroscopic approaches. However, once λ_s is known, it can provide a useful tool for correlating enzyme rate with the effect of different mutations.

1. Introduction

Hydride-transfer processes play an important role in many enzymatic reactions including dihydrofolate reductase,[1] liver alcohol dehydrogenase,[2] and lactate dehydrogenase.[3] This class of reactions can provide a useful insight about the nature of charge-transfer enzymatic reactions. For example, one would like to understand the requirements for efficient catalysis of charge-transfer reactions in general and hydride transfer in particular. Obviously this problem is not new, and previous studies of charge-transfer reactions in enzymes have indicated that enzymes catalyze such reactions by providing electrostatic complementarity

* To whom correspondence should be addressed.
† University of Southern California.
‡ University of Bristol Medical School.

(1) Thillet, J.; Adams, J. A.; Benkovic, S. J. *Biochemistry* **1990**, *29*, 5195.
(2) Scharschmidt, M.; Fisher, M. A.; Clelands, W. W. *Biochemistry* **1984**, *23*, 5471.
(3) Holbrook, J. J.; Liljas, A.; Steindel, S. J.; Rossmann, M. G. In *The Enzymes*, 3rd ed.; Boyer, P. D., Ed.; Academic Press: New York, 1975; Vol. XI, p 191.

0002-7863/91/1513-4800$02.50/0